

NEXT: results from NEXT-White and roadmap toward the $\beta\beta^{0\nu}$ search

P. Novella^{*†}

Instituto de Física Corpuscular, IFIC (CSIC & UV), 6980 Paterna, Spain

E-mail: pau.novella@ific.uv.es

The goal of the NEXT (Neutrino Experiment with a Xenon TPC) collaboration is the sensitive search of the neutrino-less double beta decay ($\beta\beta^{0\nu}$) of ^{136}Xe at the Laboratorio Subterráneo de Canfranc (LSC). The observation of such a lepton-number-violation process would prove the Majorana nature of neutrinos, providing also handles for an eventual measurement of the neutrino absolute mass. After a successful R&D phase, a first large-scale prototype of a high-pressure gas-Xenon electroluminescent TPC is being operated at the LSC since 2016. NEXT-White is a 5-kg radiopure detector meant to understand the relevant backgrounds for the $\beta\beta^{0\nu}$ search and to perform a measurement of the two neutrino mode of the double beta decay ($\beta\beta^{2\nu}$). The operation of NEXT-White is setting the grounds for the construction of the NEXT-100 detector: a TPC holding 100 kg of ^{136}Xe and reaching a sensitivity to the $\beta\beta^{0\nu}$ half-life of 6×10^{25} y after 3 years of data taking. In this document, the latest results from the NEXT-White detector are presented. The calibration data have allowed to evaluate the performance of the NEXT technology in terms of the topology-based background rejection capabilities and the energy resolution. In particular, a world-leading resolution for a Xe TPC has been achieved ($<1\%$ FWHM at 2.6 MeV). The radioactivity-induced backgrounds have also been measured using the data collected operating the detector with depleted xenon. These results validate the background model of the NEXT experiment, estimating less than 5×10^{-4} counts/keV/kg/year in the NEXT-100 detector. As NEXT-White is currently taking data with ^{136}Xe , preliminary results on the measurement of the $\beta\beta^{2\nu}$ half-life are released. Finally, the status of NEXT-100 and future upgrades, like the Ba^{++} tagging R&D, are also addressed.

*European Physical Society Conference on High Energy Physics - EPS-HEP2019 -
10-17 July, 2019
Ghent, Belgium*

^{*}Speaker.

[†]For the NEXT collaboration.

1. Searching for the $\beta\beta^{0\nu}$ decay with a high-pressure Xe TPC

The search for the neutrinoless double beta decay ($\beta\beta^{0\nu}$) implies a significant experimental challenge that needs to be addressed in terms of a good energy resolution, extra handles to identify background events, and radiopure and scalable detector technologies. The technological approach adopted by the NEXT collaboration is a high-pressure (10–15 bar) gaseous xenon time projection chamber (TPC) [1]. ^{136}Xe is known to be a suitable isotope for the $\beta\beta^{0\nu}$ search due to its relatively high $Q_{\beta\beta}$ (~ 2.5 MeV) and the long half-life of the two neutrino mode ($\beta\beta^{2\nu}$), among other reasons. Xenon is also a good detection material due to its scintillation properties. Charged particles interacting in the TPC active volume produce both primary scintillation light (S1) and ionization electrons. The ionization charge is drifted to the anode, where secondary scintillation (S2) is produced by means of the electroluminescence process (EL) in a few mm gap with a higher electric field. The S1 light is collected by an array of low-radioactivity photomultipliers (PMTs) located behind a transparent cathode (*energy plane*), providing the initial time of the event (t_0). The S2 light is detected by the same readout plane allowing for a precise determination of the total energy of the event, as well as by a dense array of silicon photomultipliers (SiPMs) located behind the anode (*tracking plane*). These SiPMs also provide the topological signature of the event.

2. The NEXT-White detector at the LSC

NEXT-White is the first radiopure implementation of the NEXT TPC. It was installed in 2015 at the Laboratorio Subterráneo de Canfranc (LSC) and has been in stable operation since 2016. The main scientific goals of NEXT-White are the technology certification for the NEXT-100 detector, the validation of the NEXT background model, and a measurement of the ^{136}Xe $\beta\beta^{2\nu}$ decay mode. Its active volume is 530.3 mm along the drift direction, with a 198 mm radius. The energy plane read-out consists of 12 Hamamatsu R11410-10 PMTs. The tracking plane read-out consists of 1792 SensL C-Series SiPMs. In order to reduce the external backgrounds, a 6 cm thick copper shield within the pressure vessel has been installed. A schematic view of the detector is shown in Fig.1. The detector lies on a seismic platform and is surrounded by two additional shield structures made of lead bricks (inner and outer lead castles), providing further shielding against external backgrounds. A radon abatement system (RAS) by ATEKO A.S. is flushing radon-free air into the air volume enclosed by the outer lead castle since October 2018. This system reduces by 4–5 orders of magnitude the ^{222}Rn content in the LSC Hall A air [3], allowing for the operation of the detector in a virtually radon-free environment.

The detector was operated with ^{136}Xe -depleted xenon ($\simeq 3\%$ isotopic abundance) between October 2016 and January 2019 (Run I–IV), and has been operating with ^{136}Xe -enriched xenon ($\simeq 91\%$ isotopic abundance) since February 2019 (Run-V). The detector conditions during Run-IV (devoted to background measurement) and Run-V (devoted to the $\beta\beta^{2\nu}$ measurement) are the same: the gas pressure, drift field and EL field are set to 10.1 bar, 0.4 kV/cm and 1.7 kV/(cm·bar), respectively. The electron drift velocity is measured to be 0.92 mm/ μs [4], while the gas purity has been continuously improving with time (electron drift lifetime ~ 5000 μs at the end of Run-IV) due to the recirculation through a heated getter-based purifier MonoTorr PS4-MT50-R from SAES. Continuous detector calibration and monitoring is carried out with a $^{83\text{m}}\text{Kr}$ low-energy

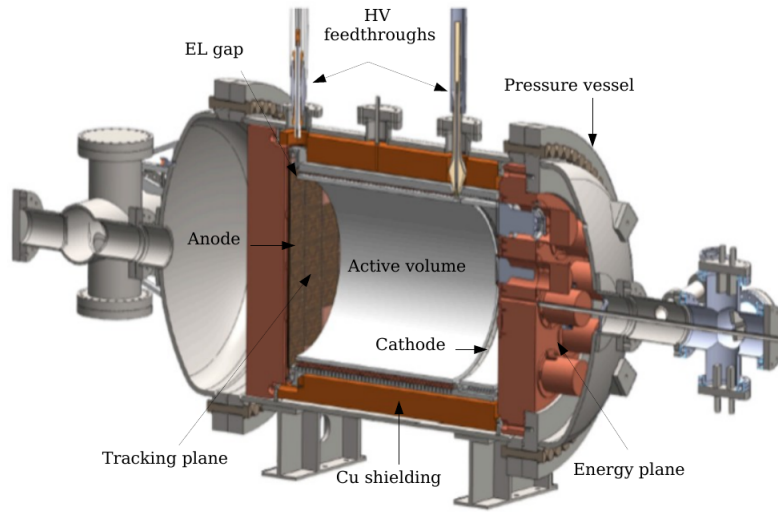


Figure 1: Schematic view of the NEXT-White detector and its main components.

calibration source, ensuring high-quality and properly calibrated low-background data [5]. Regular high-energy calibration campaigns, deploying ^{137}Cs and ^{228}Th sources, are performed in order to calibrate the detector energy scale, to measure the energy resolution at different energies, and to validate the event selection efficiencies of low-background data.

3. Energy resolution and background rejection

The events collected with the NEXT-White detector are reconstructed as follows. First, the PMT waveforms are processed to zero-suppress the data and to find the S1 and S2 signals. Then, the SiPM hits providing the X and Y coordinates are reconstructed separately for each time (or z) slice of the S2 signals. To determine the total energy of the event, the PMT charge associated to each reconstructed 3D hit in the event is separately corrected for electron attachment. The electron lifetime assumed for the correction is derived from the ^{83m}Kr data collected within a ~ 24 -hour period, where time variations are also taken into account. In addition, a geometrical correction of the detector response depending on the hit xy position is also applied. The correction relies on a xy energy map obtained also from the ^{83m}Kr data within the same 24-hour period.

The high energy calibration data are used to measure the energy resolution at 662 keV (^{137}Cs photo-peak), 1592 keV (^{208}Tl double-escape peak) and 2615 keV (^{208}Tl photo-peak). The corresponding resolutions are shown in Fig. 2[6]. A resolution better than 1% FWHM is obtained at 2615 keV (above ^{136}Xe $Q_{\beta\beta}$), as predicted in the preceding study [7]. This resolution is achieved over nearly the entire active volume, demonstrating the effectiveness of the continuous ^{83m}Kr -based calibration procedure. This result also establishes the NEXT technology (electroluminescent high pressure xenon TPC) as the one with the best energy resolution of all xenon detectors for $\beta\beta^{0\nu}$ searches.

Beyond the good energy resolution, the topological signature of the events provides a powerful handle for background rejection. Once the 3D hits are grouped into tracks, it is possible to

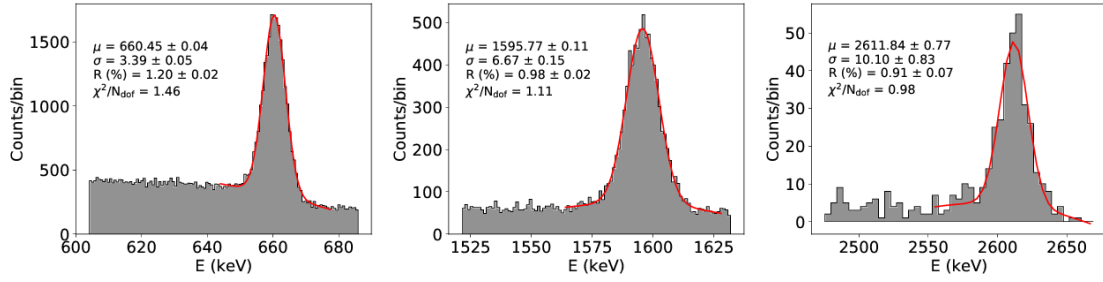


Figure 2: Energy resolutions obtained from the ^{137}Cs photo-peak (left), ^{208}Tl double-escape peak (middle), and ^{208}Tl photo-peak (right).

discriminate between single-electron (background) and double-electron (signal-like) events. While single-electrons show a larger energy deposition in one of the track extremes (where the electron comes to rest), double-electron tracks exhibit energy *blobs* at both extremes. As described in [8], ^{208}Tl calibration data have been used to obtain signal-like events (electron-positron pairs) and background-like events (single e^- from Compton interactions) at the same energy (~ 1.6 MeV). Applying an energy threshold of 266 keV for the identification of the blobs at the end of the tracks (see left panel of Fig. 3), a signal detection efficiency of $71.6 \pm 1.5_{stat} \pm 0.3_{sys}\%$ is obtained for a background acceptance of $20.6 \pm 0.4_{stat} \pm 0.3_{sys}\%$ (right panel of Fig. 3). The results derived from the data are consistent with a Monte-Carlo simulation, and improve those reported in [9]. The simulation yields further improvement at the $Q_{\beta\beta}$ of ^{136}Xe : a signal efficiency of $71.5 \pm 0.1_{stat} \pm 0.3_{sys}\%$ is obtained for a background acceptance of $13.6 \pm 1.1_{stat} \pm 0.7_{sys}\%$.

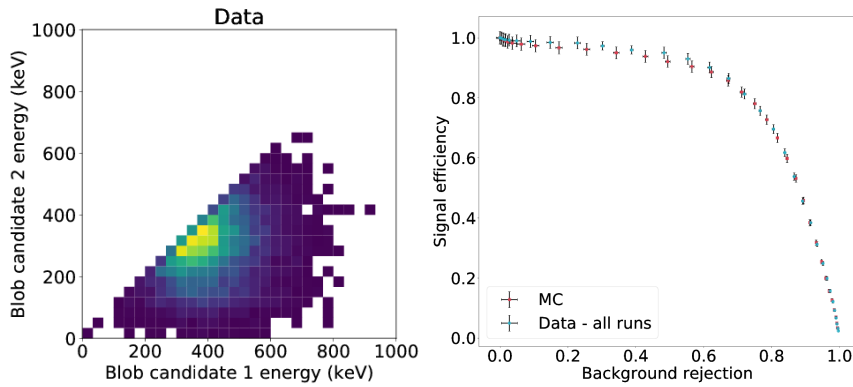


Figure 3: Topological selection. Left: distribution of the energies at both extremes of double-electron tracks from ^{208}Tl data. Right: signal efficiency as a function of background rejection, varying the energy threshold defining the blobs.

4. Radiogenic background measurement

The radioactivity-induced background in NEXT has been measured in [10] using Run-IV data. The background rate in the fiducial volume of NEXT-White is found to be $2.78 \pm 0.03_{stat} \pm 0.03_{sys}$

mHz above 600 keV. The energy spectrum has been compared to a radiogenic background model built upon an extensive radiopurity measurements campaign [11, 12, 13]. The model considers four isotopes (^{214}Bi , ^{208}Tl , ^{40}K and ^{60}Co) and 44 detector materials, which can be grouped into three effective volumes (cathode region, anode region, and any other region). In order to normalize the different contributions to the background model, an effective fit to the Run-IV data has been performed in the 1000–3000 keV range. The fit considers both the energy and the z (drift) coordinate of the events, yielding best-fit values and errors for 12 parameters: the contributions of the four isotopes in the three effective volumes. The results are shown in Fig.4, in terms of the total ^{214}Bi , ^{208}Tl , ^{40}K and ^{60}Co background rates. Summing over all isotopes, the overall scale factor of the expected total rate is 1.72 ± 0.04 with respect to the nominal background prediction. According to the fit results, the observed excess is mostly due to the ^{60}Co contribution from the anode region, which is currently under investigation.

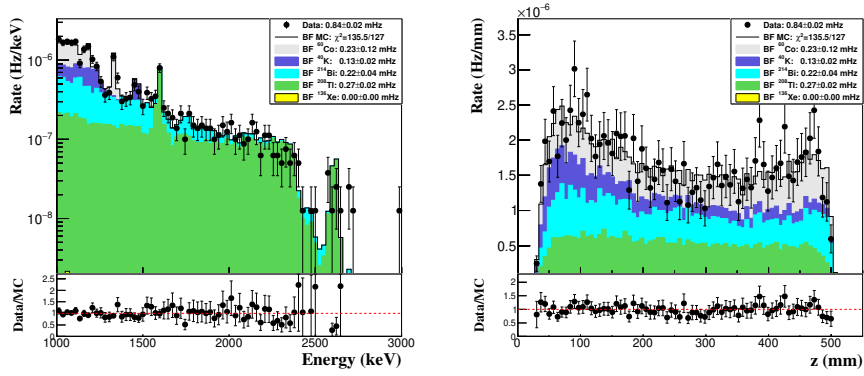


Figure 4: Background measurement. Data (black dots) are superimposed to the best-fit background model expectation (solid histograms), for which the different isotopes contributions are shown. The displayed isotope rates are obtained by propagating the best-fit values of the three effective volumes for each isotope.

In order to evaluate the backgrounds in $\beta\beta$ analyses, the double-electron selection cuts previously described are applied to the Run-IV fiducial data and MC background samples, once rescaled by the best-fit values of the fit. The corresponding background spectra is shown in Fig. 5. The consistency between the rates in data and MC ensures the validity of the background model also after the topological selection. A total background rate above 1000 keV of 0.248 ± 0.010 mHz is observed, for an expectation of $0.246 \pm 0.001_{stat} \pm 0.008_{sys}$ mHz. In particular, the background expectation is also consistent with data in a $Q_{\beta\beta} \pm 100$ keV window. The background rejection factor due to the double-electron selection, with respect to the fiducial sample, is found to be about 3.4 for $E > 1000$ keV, and about 17 in the $Q_{\beta\beta} \pm 100$ keV range.

5. Measurement of the $\beta\beta 2\nu$ decay with NEXT-White

The ongoing Run-V (^{136}Xe -enriched operation) data taking will allow for the measurement of the $\beta\beta^{2\nu}$ half-life ($T_{1/2}^{2\nu}$). The first double-electron tracks from the ^{136}Xe double beta decay have been observed. As an example, left panel of Fig. 6 shows a reconstructed (Lucy-Richardson deconvolution) $\beta\beta$ track of 2.1 MeV, with two clear energy blobs at the extremes. According to the

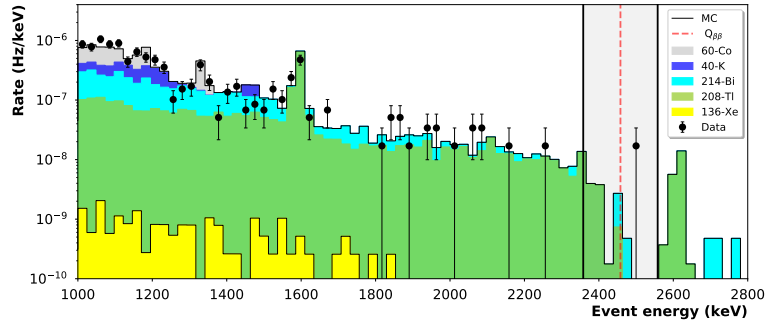


Figure 5: $\beta\beta$ background: energy spectrum after topological cuts are applied to background MC and Run-IV data. The light grey band shows the $Q_{\beta\beta} \pm 100$ keV window considered to compare the data to the MC expectation around $Q_{\beta\beta}$.

rescaled MC background model and the current topological selection, a $(3.5 \pm 0.6)\sigma$ measurement of $T_{1/2}^{2\nu}$ can be achieved in NEXT-White after 1 year [10]. The operation of NEXT-White with enriched xenon will continue until summer 2020, when the installation of NEXT-100 starts. Accounting for the current DAQ dead-time in Run-V, a total live time of about one year is expected. However, a preliminary $\beta\beta^{2\nu}$ analysis has been performed with the first 78 days of Run-V. The data have been fitted to the background model plus a $\beta\beta^{2\nu}$ MC, accounting for both Run-IV and Run-V samples. As done for the Run-IV background fit, the energy and the spatial distribution of the events have been considered. The results are shown in the right panel of Fig. 6, where the best-fit values for the background and the ^{136}Xe contributions are displayed.

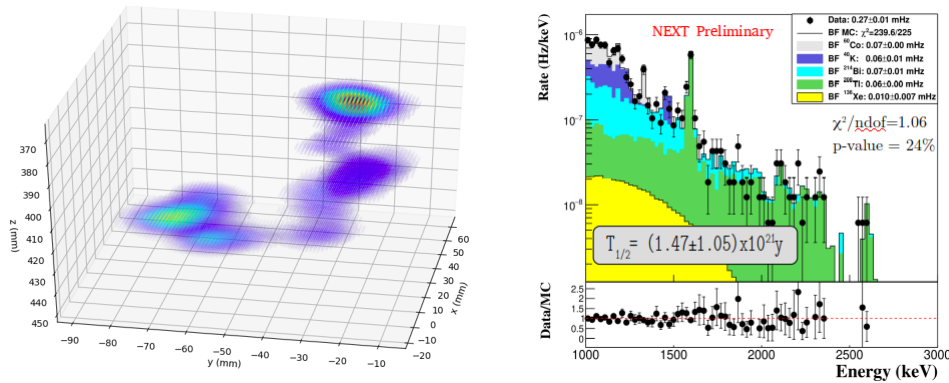


Figure 6: Preliminary $\beta\beta^{2\nu}$ results. Left: $\beta\beta$ track of 2.1 MeV, reconstructed with a Lucy-Richardson deconvolution algorithm. Right: preliminary $T_{1/2}^{2\nu}$ measurement using Run-IV data and the first 78 days of Run-V.

6. Search for the $\beta\beta 0\nu$ decay: NEXT-100 and beyond

The technology of NEXT-White is being scaled up in order to build the NEXT-100 detector at

the LSC, holding 100 kg of ^{136}Xe . The installation will start in 2020. By means of Monte Carlo techniques (validated with NEXT-White), the background rejection factors for the different event selection cuts have been computed. According to these factors and the NEXT background model, the final expected background index in NEXT-100 is $\sim 5 \times 10^{-4}$ counts/keV·kg·year. This value can be further reduced by means of better reconstruction algorithms [14] and track identification techniques based on deep neural networks [15]. This very low background rate will allow the NEXT-100 detector to reach a sensitivity to the $\beta\beta^{0\nu}$ half-life of $T_{1/2}^{0\nu} > 6.0 \times 10^{25}$ year (90% C.L) for an exposure of 300 kg·year ($\langle m_\nu \rangle = 70\text{-}130$ meV depending on the nuclear matrix elements considered).

Beyond the operation of NEXT-100, the NEXT collaboration is already working on the design of detectors in the ton-scale. An incremental approach has been defined to develop upgrades to the current technology and the corresponding R&D program has already started. The first step considers the replacement of the PMTs by SiPMs (more radiopure and better light collection), and the operation at cooler temperatures (reduced dark count rate) and with low diffusion gas mixtures (improvement of the topological signature). The second step considers the implementation of ^{136}Ba -tagging capabilities based on single-molecule fluorescence imaging [16].

References

- [1] V. Alvarez *et al.*, JINST **7** (2012) T06001 [arXiv:1202.0721 [physics.ins-det]].
- [2] F. Monrabal *et al.*, JINST **13** (2018) no.12, P12010 [arXiv:1804.02409 [physics.ins-det]].
- [3] P. Novella *et al.*, JHEP **1810** (2018) 112 [arXiv:1804.00471 [physics.ins-det]].
- [4] A. Simón *et al.*, JINST **13** (2018) no.07, P07013 [arXiv:1804.01680 [physics.ins-det]].
- [5] G. Martínez-Lema *et al.*, JINST **13** (2018) no.10, P10014 [arXiv:1804.01780 [physics.ins-det]].
- [6] J. Renner *et al.*, arXiv:1905.13110 [physics.ins-det].
- [7] J. Renner *et al.*, JINST **13** (2018) no.10, P10020 [arXiv:1808.01804 [physics.ins-det]].
- [8] P. Ferrario *et al.*, arXiv:1905.13141 [physics.ins-det].
- [9] P. Ferrario *et al.*, JHEP **1601** (2016) 104 [arXiv:1507.05902 [physics.ins-det]].
- [10] P. Novella *et al.*, arXiv:1905.13625 [physics.ins-det].
- [11] V. Alvarez *et al.*, JINST **8** (2013) T01002 [arXiv:1211.3961 [physics.ins-det]].
- [12] S. Cebrián *et al.*, JINST **12** (2017) no.08, T08003 [arXiv:1706.06012 [physics.ins-det]].
- [13] S. Cebrián *et al.*, JINST **10** (2015) no.05, P05006 [arXiv:1411.1433 [physics.ins-det]].
- [14] A. Simón *et al.*, JINST **12** (2017) no.08, P08009 [arXiv:1705.10270 [physics.ins-det]].
- [15] J. Renner *et al.*, JINST **12** (2017) no.01, T01004 [arXiv:1609.06202 [physics.ins-det]].
- [16] A. D. McDonald *et al.*, Phys. Rev. Lett. **120** (2018) no.13, 132504 [arXiv:1711.04782 [physics.ins-det]].